Removal of Pb(II) from Aqueous Solutions by Zeolites, Porcelanite and Sands: Correlation of Morphology and Chemical Composition to Batch Removal Efficiency

Fawwaz Jumean[1*], Lucia Pappalardo[1], Hani Khoury[2]

[1]Department of Biology, Chemistry and Environmental Sciences, American University of Sharjah, Sharjah, United Arab Emirates
[2]Department of Geology, The University of Jordan, Amman, Jordan
Email: *fjumean@aus.edu

Abstract

Chemical compositions of natural zeolites, porcelanite (opal-CT) and local sands were determined by X-ray fluorescence (XRF) and correlated with their Pb(II) removal efficiencies. Zeolites and porcelanite were from the Mikawer, Aritain and Hannon areas in Jordan. Sands (white, red and yellow) were from the United Arab Emirates (UAE). The effect of Pb(II) concentration and zeolite dosage on removal efficiency was investigated at $25.0°C$ using the batch equilibrium method. Commercial kaolinite, silica and alumina were also studied for comparison. Removal efficiencies, in mg Pb(II)/g adsorbent, were: 76.9, 52.7 and 42.1 for Hannon, Mikawer and Aritain zeolites, respectively; 58.2 for porcelanite; 29.7, 11.0 and 8.5 for yellow, red and white sand, respectively; 7.2, 3.3 and 1.3 for kaolinite, silica and alumina, respectively. XRF data indicate that adsorbents with intermediate molar ratios of Si/Al, in the range 2.70 - 2.93, are most efficient in Pb(II) removal. Scanning electron microscope (SEM) images of adsorbents suggest that morphology, in addition to chemical composition, plays a key role. In particular, a combination of factors, including shapes and sizes of crystals, channels in zeolites and pores in porcelanite, appear to favor removal of Pb(II).

Keywords

Zeolites, Sands, XRF, SEM, Pb(II) Removal

---

*Corresponding author.

1. Introduction

Pb(II) in the environment has a high level of toxicity and poses a serious hazard to human and animal health. Effluents from battery and electronics factories augment the concentration of Pb(II) in reservoirs and wastewaters. Column filtration and batch equilibrium by low cost adsorbents are the most common methods used in removing Pb(II) and other toxic heavy metals from wastewaters. UAE sands were shown to be efficient adsorbents for the removal and recovery of Pb(II) and other heavy metals from aqueous solutions [1] [2], and for the removal and speciation of Cr(III) and Cr(VI) [3] [4]. Reports on heavy metal removal from solutions by sawdust [5], eggshell [6], bentonite, molasses and fly ash [7] have also included X-ray fluorescence (XRF) data on these adsorbents. Scanning electron microscope (SEM) images have been employed in assessing adsorptive surfaces and are now regularly featured in reports on the removal of heavy metals by a variety of surfaces [8]-[11]. Heavy metals removal efficiency by montmorillonitic and calcareous clays has been correlated to the amount of calcium carbonates present in the samples [12]. Zeolites have been successfully used to remove uranium (IV) from contaminated waters [13] and oil from palm oil mill effluent [14].

Natural zeolites are considered low cost resources. They are crystalline hydrated aluminosilicates with a framework structure containing pores occupied by water, alkali and alkaline earth cations. Their tetrahedral sieve-like structure carries a negative charge due to replacement of some of aluminum by silicon. The negative charge is balanced by cations, such as sodium, calcium, potassium, or magnesium. Zeolites can lose most of their loosely bound water molecules without affecting the integrity of their molecular structure. They have high cation exchange capacity and display good selectivity for heavy metal cations that enable them to be used for the purification of industrial wastewater. Volcaniclastic rocks in Jordan are developed from cinder stratovolcanoes and are characterized by the presence of rich zeolitized beds. The zeolitization of these rocks is a function of high porosity, permeability and arid climate [15]. The open hydrological system enables the circulation of water that allows the neoformation of zeolites. In this work removal efficiencies of Pb(II) from aqueous solutions by porcelanite and zeolites from the Jordanian areas of Mikawer, Aritain and Hannon were investigated. Removal by commercial kaolinite, alumina and silica was also studied for comparison. Efficiencies using zeolites were then compared to those for white, yellow and red UAE sands, and correlated with XRF data and SEM micrographs. For each adsorbent, efficiencies were studied as a function of adsorbent dosage for several initial Pb(II) concentrations, using the batch equilibrium method. XRF and SEM studies were conducted on all adsorbents. The results allow for a preliminary correlation of chemical compositions and morphology of adsorbents with their Pb(II) removal efficiency.

2. Materials and Methods

2.1. Adsorbents and Reagents

White, yellow and red sand samples were collected from several locations in the UAE. White sand is most commonly found close to the seashore (composed mainly of rhombic calcite) whereas yellow and red sands are in the inland desert. The yellow and red colors of the particles are related to the presence of iron oxides coating. Mikawer, Aritain and Hannon zeolites were obtained from areas with the same names in Jordan. Porcelanite was obtained from the Azraq area in Jordan. Kaolin, a hydrated aluminum silicate, was lot #120M0110V, from Sigma Aldrich (USA). Alumina was from Riedel-de-Haen (Germany) and silica was from Sharlau (Spain). Zeolites were pulverized to a fine powder. Sand and zeolite samples were washed repeatedly with deionized distilled water, dried to a constant weight at 110°C then passed through a 300 μm sieve.

All primary chemicals used were of analytical reagent grade. $Pb(NO_3)_2$, NaOH and HNO_3 were from Panreac (Spain).

2.2. Instrumentation

Pb(II) concentrations were determined using a Varian Liberty axial sequential inductively coupled plasma-atomic emission spectrometer "ICP-AES" (Australia). pH was measured on a 550A Thermo Orion pH meter (USA) fitted with a combined glass electrode. Solutions were shaken at 25.0°C using an Edmund Buhler KS-15/TH-15 shaker (Germany). Sand and zeolite samples were sieved using impact test sieves from Standard Sieve (USA), mesh model BS410, 1986 ST. Three brass frames with sieve sizes 300, 150 and 75 μm were employed.

Fraction selected for experiments were less than 300 µm in diameter.

XRF images and spectra were obtained using a Horiba, XGT-7200V X-ray analytical microscope with silicon drift detector (SDD). Intensity measurements of compressed powdered samples were conducted using a tube voltage of 50 kV and an automatic tube current of 1 mA max with acquisition time of 60 s. Detected elements were Al, Si, K, Ca, Ti, Sr, S, Cl, Mg, Cr, V, Mn, Br, and Fe. Adsorbent images were taken using a charge-coupled device (CCD) as the X-ray detector. The CCD had a 100-fold magnifying scale.

SEM micrographs on sands were obtained using a high resolution TESCAN Vega 3-LMU, equipped with a 4-lens electron optics system and has a magnification range 2.5 - 1,000,000. Micrographs on platinum coated samples of zeolites and porcelanite were obtained using an FEI-INSPECT-F50, equipped with high resolution Schottky field emission (FEG), with magnification up to nano size.

2.3. Batch Studies

Batch equilibration studies on sand were performed using 0.100 dm^3 Pb(II) solutions. Initial Pb(II) concentrations were 300 ppm for all adsorbents. Additional removal experiments were carried out using 30 ppm solutions on alumina and silica, and 1000 ppm solutions on zeolites. Runs were conducted in triplicates. A known mass of adsorbent was added to Pb(II) solutions, the pH adjusted to the optimal removal value of 4.0 using 1.0 mol dm^{-3} HNO$_3$, then equilibrated at 25.0°C for 2 h at 200 rpm. Final Pb(II) concentrations were determined by ICP. Prolonging the contact time between adsorbent and solution beyond 2 h did not result in further removal of Pb(II).

3. Results and Discussion

3.1. Removal Efficiencies

The dependence of Pb(II) removal efficiency for 300 ppm solutions on adsorbent dosage is shown in **Figure 1**. It is apparent that zeolites and porcelanite are highly efficient in removing Pb(II) from aqueous solutions. Zeolite efficiencies follow the order Hannon > Mikawer > Aritain and that for porcelanite is second to Hannon. The three zeolites, porcelanite and yellow sand are capable of completely removing lead from solutions containing 300 ppm Pb(II) at adsorbent dosages in the range 0.6 - 1.0 g/0.100 dm^3. Other adsorbents are less efficient and follow the order white sand > red sand > kaolinite > silica > alumina. The maximum removal capacity of each adsorbent, defined as lead removed (mg) per g adsorbent, is reported in **Table 1**.

White and red sands are also capable of completely removing Pb(II), but only at significantly higher adsorbent dosages (2). For kaolinite, silica and alumina, 100% removal efficiencies could only be attained with low (30 ppm) Pb(II) concentrations and at adsorbent dosages higher than 3.0 g/0.100 dm^3.

High removal efficiencies with zeolites was observed even for 1000 ppm Pb(II) solutions. At this concentration, 100% removal was attained with zeolite dosages above 2.5 g/0.100 dm^3. Maximum adsorbent capacities for
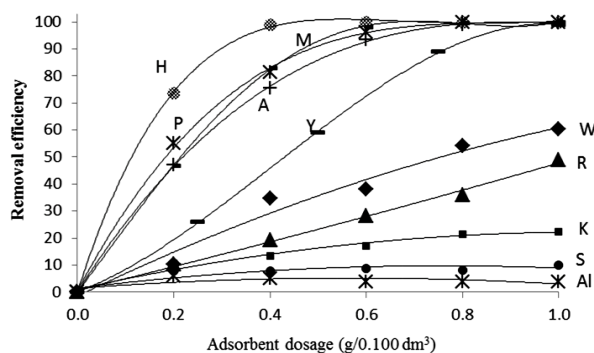

Figure 1. Pb(II) removal efficiency as a function of adsorbent dosage. Volume of solution = 0.100 dm^3. Initial [Pb(II)] = 300 ppm. T = 25.0°C. Equilibration time = 2 h. (Symbols: H = Hannon, P = porcelanite, M = Mikawer, A = Aritain, Y = yellow sand, W = white sand, R = red sand, K = kaolinite, S = silica, Al = alumina).

Pb(II) are shown in **Table 1**. The results suggest that intermediate Si/Al ratios, in the range 2.70 - 2.93, listed in **Table 3**, correspond to optimal efficiency for this class of adsorbers.

3.2. Sampling and Characterization

Zeolite tuff locations are given in **Table 2**. All samples are hypohyaline grey, red to light brown in color with rounded vesicles of different sizes. Most of the vesicles are partially filled with secondary zeolites. Calcite occurs partially as a filling material in the vesicles and between zeolites. X-ray diffraction analysis proved the presence of smectite as an alteration products of the tuffaceous material (balsatic in composition) [16]. All sam-

Table 1. Maximum Pb(II) adsorbent capacities.

Adsorbent	mg Pb/g adsorbent
Hannon	76.9 ± 2.3
Mikawer	52.7 ± 1.6
Aritain	42.1 ± 1.3
Porcelanite	58.2 ± 1.6
Yellow sand	29.7 ± 0.9
Red sand	11.0 ± 0.4
White sand	8.5 ± 0.3
Kaolinite	7.2 ± 0.2
Silica	3.3 ± 0.1
Alumina	1.3 ± 0.1

Table 2. Zeolitic tuff locations in Jordan.

Locality	Latitude (E)	Longitude (N)
Mikawer	35°42'17"	31°36'06"
Aritain	36°51'23"	32°04'44"
Hannon	37°37'44"	32°23'15"

Table 3. XRF composition data, reported as w/w% of mineral oxides and bulk molar ratio of Si/Al.

|	UAE Sands			Zeolites			Kaolinite
	Yellow	White	Red	Hannon	Mikawer	Aritain	
SiO_2	28.8	18.6	49.6	45.0	46.5	46.7	61.0
K_2O	0.91	0.81	0.97	1.01	1.29	1.45	0
CaO	46.7	70.4	22.7	8.26	8.60	8.43	0
TiO_2	0.18	0.12	0.12	3.06	3.54	2.55	1.35
Fe_2O_3	1.25	0.80	1.19	17.92	17.3	14.4	0.67
SrO	0.20	1.09	0.05	0.11	0.14	0.10	0
Al_2O_3	8.36	5.22	9.00	13.8	14.6	14.9	37.0
MgO	12.9	0	16.0	10.5	7.58	10.6	0
Si/Al	2.93	3.02	4.68	2.77	2.70	2.66	1.40

ples contain phillipsite which occurs as colorless radiating aggregates in the cement and grows at the expense of the glassy matrix. Phillipsite is also found as single prismatic crystals of spherulitic texture. Chabazite occurs in Mikawer and Hannon as isolated crystals or aggregates [15]. The crystals are characterized by rhombohedral cleavage with penetration twinning and zoning and vary in size from few microns up to 200 µm. Faujasite occurs only in the Hannon zeolite, growing as an aggregate on the vesicles wall with a size range 50 - 100 µm. The crystals are octahedrons, colorless, equant and isotropic. Mikawer and Aritain samples are reddish brown due to the presence of the phillipsite-chabazite tuff. For Mikawer and Aritain, total zeolites are 57% and CEC is 140 meq/100g [17]. Hannon samples are gray faujasite-phillipsite in 6 m thick horizon, have 29% faujasite (highest in Jordan), 45% total zeolites and a CEC of 154 meq/100g [17].

Thick deposits of porcelanite (active silica) are found in northeastern Jordan (Badia region) and samples for this study were collected from the Azraq area, located within this region. Porcelanite occurs in two layers: the lower (0.6 - 1.3 m thick) is white, gray, and pink and the upper (0.4 - 0.6 m) is white-gray. The layers are separated by dark brown-black chert (5 - 15 cm) and chalk (0.6 - 1.8 m). The mineralogical composition of porcelanite is dominated by opal-CT (cristoballite-tridymite) and quartz. The SiO_2 content is >90%. The high purity of the porcelanite layers and the low iron content (average 0.06%) result in a high average whiteness index (87%) [15]. Opal-CT is poorly crystalline and its SiO_2 phase consists of partially unshared SiO_4 tetrahedra. Its broken edges and large surface area contribute to its high adsorption capacity. It has the same chemical composition as quartz (sand). Quartz is made up of SiO_4 tetrahedra shared in all directions (3-dimensional structure, with no broken edges), which explains its electrical neutrality and poor adsorption capacity [16].

3.3. XRF and SEM Measurements

Chemical compositions of zeolites, sands and kaolinite, as determined by XRF, are given in **Table 3**. Metal oxide content and the corresponding bulk molar ratios of Si/Al (number of silicon framework atoms/number of aluminum framework atoms) ratios are also shown. This ratio varies from 1.40 for kaolinite to 4.68 for red sand. The Si/Al ratio has been shown to play an important role also in the conversion of fly ash compounds into zeolites [18]. For the most efficient adsorbents, the range is narrow, 2.70 - 2.93, suggesting that very low or very high ratios inhibit removal. Pure alumina (Al_2O_3) and pure silica (SiO_2), representing both extremes of this ratio, are not efficient adsorbers. Kaolinite, with a ratio of 1.40, is also not efficient, primarily because of the electrical neutrality of the Si-tetrahedral and Al-octahedral sheets of kaolinite (two-dimensional 1:1 structure). Whereas zeolites are relatively rich in iron and sands in calcium, it is not certain how, if at all, these metals contribute to their adsorption properties. **Table 3** also shows that, with the exception of white sand, magnesium is present in fair amounts in both zeolites and sands. By contrast, white sand is exceptionally rich in lime (CaO) due to the presence of calcite ($CaCO_3$). Zeolites and kaolinite have significantly higher content of TiO_2 when compared to sands. Although porcelanite does not contain aluminum, its high adsorptive behavior is probably due to its fine size fraction and the presence of negative charge along the broken edges of the shared SiO_4 tetrahedra that form the framework structure of its SiO_2 phases [15].

SEM micrographs for the three zeolites, porcelanite and the three types of sand are presented at various resolutions in **Figures 2-4**, respectively. The micrographs show that sands have significantly larger grain size (lower porosity) than zeolites or porcelanite, with portions of the sand surfaces being very smooth. The lower porosity of sand in comparison with zeolites and porcelanite is related to the absence of adsorptive surfaces. Zeolites and porcelanite have a typical microporous texture that results from their fine crystal size (high surface areas) (**Figure 2** and **Figure 3**). **Figure 2** also shows the euhedral nature of zeolites (phillipsite). Zeolites that have a channel like structure and high cation exchange capacity (CEC) can act as molecular sieves [13]. **Figure 3** illustrates the microporous texture and large surface area of porcelanite. **Figure 4** illustrates the morphology of the three sand-silt size varieties. All sand samples have three-dimensional crystal forms. The mineralogical composition of the three types is variable as some indicate cleavage planes (**Figure 4(a)** and **Figure 4(b)**). White and yellow sands are dominated by the electrically neutral calcite ($CaCO_3$). Red sand is dominated by quartz (SiO_2) which has an electrically neutral tetrahedral network (tectosilicates) structure. Thus sands are electrically neutral and have relatively very small surface areas in comparison with zeolites, which have a high CEC, and porcelanite, which is highly microporous. This, at least in part, explains why zeolites and porcelanite are better adsorbers than sand. Nevertheless, the morphology, including channels and crevices, should be viewed in conjunction with chemical compositions of adsorber and adsorbate and the ability of the adsorber not only to accommodate the
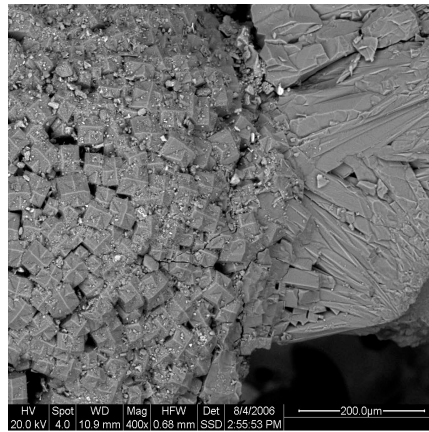
(a)
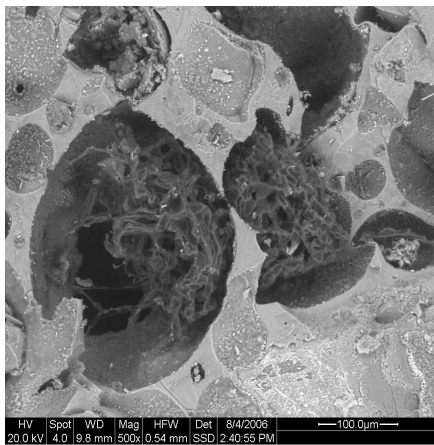
(b)
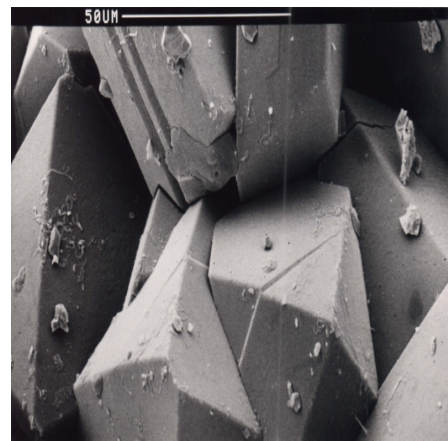
(c)

Figure 2. SEM micrographs of (a) Mikawer zeolite with phillipsite radiating and growing at the expense of the glassy matrix. (b) Aritain zeolite with rounded vesicles of different sizes filled with secondary minerals. (c) Hannon octahedral faujasite crystals.
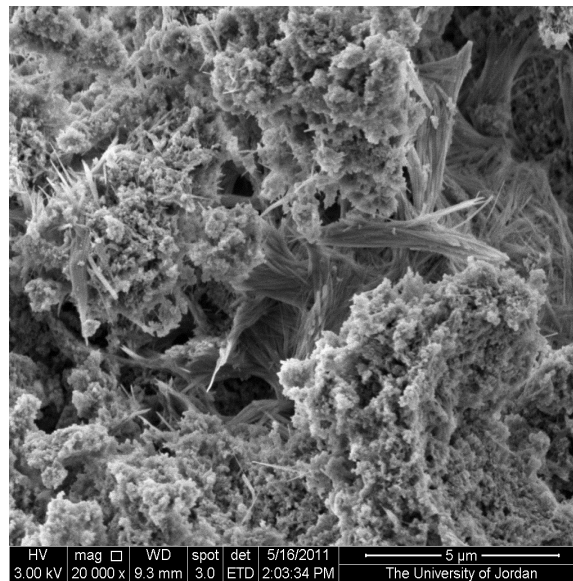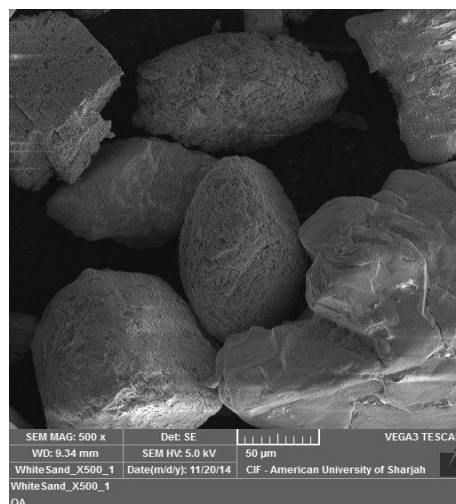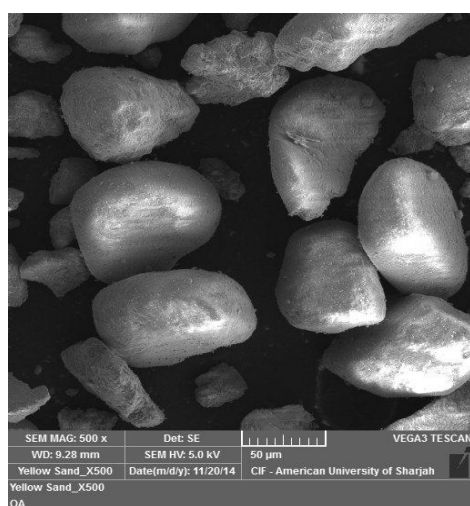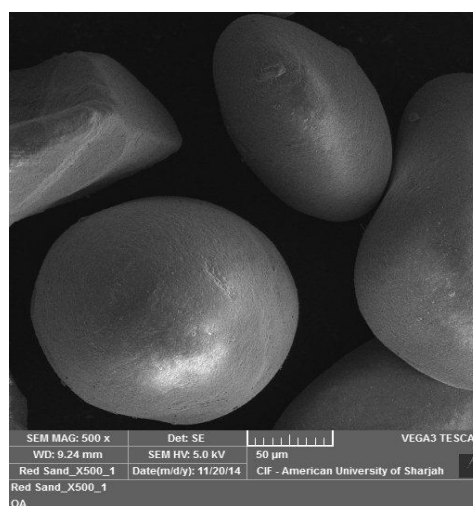

Figure 3. SEM micrograph of porous porcelanite.

(a)

(b)

(c)

Figure 4. SEM micrographs of UAE sands. (a) white; (b) yellow; (c) red.

latter within its structure but also to form strong bonds with it.

It is worthy of note that zeolites and porcelanite are significantly more efficient removers of Pb(II) than sands and this is notwithstanding the comparable Si/Al ratios of zeolites to those for white and yellow sands. The efficiency difference suggests that morphology, in addition to chemical composition, has an important role. In particular, a combination of factors, including shapes and sizes of the crystals, channels in the zeolites and pores in porcelanite investigated appear to favor accommodation of Pb(II).

4. Conclusions

In addition to investigating and comparing Pb(II) removal efficiencies by zeolites, sands and other common adsorbents, this work is a preliminary attempt to correlate these efficiencies with chemical compositions of adsorbents. Removal efficiencies, in mg Pb(II)/g adsorbent, were: 76.9, 52.7 and 42.1 for Hannon, Mikawer and Aritain zeolites, respectively; 58.2 for porcelanite; 29.7, 11.0 and 8.5 for yellow, red and white sand, respectively; and 7.2, 3.3 and 1.3 for kaolinite, silica and alumina, respectively. The bulk molar ratio of Si/Al in an adsorbent, as obtained by XRF, appears to be an efficiency indicator for sands, zeolites and other aluminum silicates.

The high removal efficiencies of zeolites and porcelanite allow for their use in municipal and industrial wastewater treatment plants. The high adsorption capacity of zeolitic tuff and porcelanite, in comparison with

sand, enables their use as filters.

Acknowledgements

References

[1] Pappalardo, L., Jumean, F. and Abdo, N. (2010) Removal of Cadmium, Copper, Lead and Nickel from Aqueous Solution by White, Yellow and Red United Arab Emirates Sand. *American Journal of Environmental Sciences*, **6**, 41-44. http://dx.doi.org/10.3844/ajessp.2010.41.44

[2] Pappalardo, L., Jumean, F. and Abdo, N. (2011) Removal and Recovery of Lead from Aqueous Solution by Low Cost Media. *American Journal of Environmental Sciences*, **7**, 141-144. http://dx.doi.org/10.3844/ajessp.2011.141.144

[3] Khamis, M., Jumean, F. and Abdo, N. (2009) Speciation and Removal of Chromium from Aqueous Solution by White, Yellow and Red UAE Sand. *Journal of Hazardous Materials*, **169**, 948-952. http://dx.doi.org/10.1016/j.jhazmat.2009.04.053

[4] Jumean, F., Khamis, M., Sara, Z. and AbouRich, M. (2015) Concurrent Removal and Reduction of Cr(VI) by Wool: Short and Long Term Equilibrium Studies. *American Journal of Analytical Chemistry*, **6**, 47-57. http://dx.doi.org/10.4236/ajac.2015.61005

[5] Bulut, Y. and Tez, Z. (2007) Removal of Heavy Metals from Aqueous Solution by Sawdust Adsorption. *Journal of Environmental Sciences*, **19**, 160-166. http://dx.doi.org/10.1016/S1001-0742(07)60026-6

[6] Park, H.J., Jeong, S.W., Yang, J.K., Kim, B.G. and Lee, S.M. (2007) Removal of Heavy Metals Using Waste Eggshell. *Journal of Environmental Sciences*, **19**, 1436-1441. http://dx.doi.org/10.1016/S1001-0742(07)60234-4

[7] Kolemen, S., Arcali, N., Tugrul, N., Derun, E. and Piskin, S. (2013) The Zinc Adsorption Study by Using Orhaneli Fly Ash, Bentonite, and Molasses in Wastewater. *Water*, *Air & Soil Pollution*, **224**, 1-10. http://dx.doi.org/10.1007/s11270-012-1367-2

[8] Yang, J., Lee, J.Y., Park, Y., Baek, K and Choi, J. (2010) Adsorption of As(III), AS(V), Cd(II), Cu(II), and Pb(II) from Aqueous Solutions by Natural Muscovite, *Separation Science and Technology*, **45**, 814-823. http://dx.doi.org/10.1080/01496391003609023

[9] Kim, J.S., Zhang, L. and Keane, M. (2001) Removal of Iron from Aqueous Solutions by Ion Exchange with Na-Y Zeolite. *Separation Science and Technology*, **36**, 1509-1525. http://dx.doi.org/10.1081/SS-100103885

[10] Zhu, Z., Li, L., Zhang, H., Qiu, Y. and Zhao, J. (2010). Adsorption of Lead and Cadmium on Ca-Deficient Hydroxyapatite. *Separation Science and Technology*, **45**, 262-268. http://dx.doi.org/10.1080/01496390903423626

[11] Shukla, S.R., Giakar, V.G., Pai, R.S. and Suryavanshi, U.S. (2009) Batch and Column Adsorption of Cu(II) on Unmodified and Oxidized Choir. *Separation Science and Technology*, **44**, 40-62. http://dx.doi.org/10.1080/01496390802281984

[12] Sdiri, A., Higashi, T., Hatta, T., Jamoussi, F. and Tase, N. (2011) Evaluating the Adsorptive Capacity of Montmorillonitic and Calcareous Clays on the Removal of Several Heavy Metals in Aqueous Systems. *Chemical Engineering Journal*, **172**, 37-46. http://dx.doi.org/10.1016/j.cej.2011.05.015

[13] Camacho, L.M., Deng, S. and Parra, R.R. (2010) Uranium Removal from Groundwater by Natural Clinoptilolite Zeolite: Effects of pH and Initial Feed Concentration. *Journal of Hazardous Materials*, **175**, 393-398. http://dx.doi.org/10.1016/j.jhazmat.2009.10.017

[14] Shavandi, M.A., Haddadian, Z., Ismail, M.H.S., Abdullah, N. and Abidin, Z.Z. (2012) Removal of Residual Oils from Palm Oil Mill Effluent by Adsorption on Natural Zeolite. *Water*, *Air & Soil Pollution*, **223**, 4017-4027. http://dx.doi.org/10.1007/s11270-012-1169-6

[15] Khoury, H. (2006) Industrial Rocks and Minerals in Jordan. 2nd Edition, University of Jordan Press, Amman.

[16] Yousef, R., El-Eswed, B., Alshaaer, M., Khalili, F. and Khoury, H. (2009) The Influence of Using Jordan Zeolites on the Adsorption, Physical, and Mechanical Properties of Geopolymers Products. *Journal of Hazardous Materials*, **165**, 379-387. http://dx.doi.org/10.1016/j.jhazmat.2008.10.004

[17] Khoury, H., Ibrahim, K., Ghrir, A. and Ed-Deen, T. (2003) Zeolites and Zeolitic Tuff in Jordan. University of Jordan Press, Amman.

[18] Somerset, V.S., Petrik, L.F., White, R.A., Klink, M.J., Key, D. and Iwuoha, E. (2004) The Use of X-Ray Fluorescence (XRF) Analysis in Predicting the Alkaline Hydrothermal Conversion of Fly Ash Precipitates into Zeolites. *Talanta*, **64**, 109-114. http://dx.doi.org/10.1016/j.talanta.2003.10.059